Review of Scientific Instruments

In-circuit-measurement of parasitic elements in high gain high bandwidth low noise transimpedance amplifiers

Cite as: Rev. Sci. Instrum. **85**, 124703 (2014); https://doi.org/10.1063/1.4902854
Submitted: 15 May 2014 . Accepted: 15 November 2014 . Published Online: 08 December 2014

P. Cochems, A. Kirk, and S. Zimmermann

In-circuit-measurement of parasitic elements in high gain high bandwidth low noise transimpedance amplifiers

P. Cochems, A. Kirk, and S. Zimmermann
Institute of Electrical Engineering and Measurement Technology, Department of Sensors and Measurement Technology, Leibniz University Hannover, Hannover, Germany

(Received 15 May 2014; accepted 15 November 2014; published online 8 December 2014)

Parasitic elements play an important role in the development of every high performance circuit. In the case of high gain, high bandwidth transimpedance amplifiers, the most important parasitic elements are parasitic capacitances at the input and in the feedback path, which significantly influence the stability, the frequency response, and the noise of the amplifier. As these parasitic capacitances range from a few picofarads down to only a few femtofarads, it is nearly impossible to measure them accurately using traditional LCR meters. Unfortunately, they also cannot be easily determined from the transfer function of the transimpedance amplifier, as it contains several overlapping effects and its measurement is only possible when the circuit is already stable. Therefore, we developed an in-circuit measurement method utilizing minimal modifications to the input stage in order to measure its parasitic capacitances directly and with unconditional stability. Furthermore, using the data acquired with this measurement technique, we both proposed a model for the complicated frequency response of high value thick film resistors as they are used in high gain transimpedance amplifiers and optimized our transimpedance amplifier design. © *2014 AIP Publishing LLC*. [http://dx.doi.org/10.1063/1.4902854]

I. INTRODUCTION

Transimpedance amplifiers are used to convert low currents into usable voltage signals, which is required in a variety of sensor applications. Often, the performance of the transimpedance amplifier can become a limiting factor for the overall performance of the measurement system. One example for such a case from our field of work are time-of-flight ion mobility spectrometers (TOF-IMS), which use a faraday plate to collect ions after a transient ion separation within an electric drift field under atmospheric pressure.[1] The ion currents to be measured are rather low, with typical peak values ranging from a few tens of picoamperes to one nanoampere, thus requiring high gain of several gigaohms. At the same time, the transient nature of the measurement signal both requires an amplifier bandwidth of more than 100 kHz to separate the different peaks[2] and low noise to achieve a high signal-to-noise ratio within few measurement repetitions. This combination creates demanding requirements on the performance of the employed transimpedance amplifiers, resulting in complex designs and therefore necessitating sophisticated tools for their development.

II. TRANSFER FUNCTION AND STABILITY

The typical transimpedance amplifier configuration using an operational amplifier (OP) is shown in Figure 1. Due to the infinitesimal low voltage between the differential inputs of the operational amplifier, the inverting input is kept close to ground. As the input current I_{in} cannot flow into the operational amplifier's input due to its high input impedance,[3] it has to flow through the feedback resistor R_f, resulting in an output voltage V_{out} of the operational amplifier. In the alternating current case, this output voltage is dependent on several parasitic effects. First, the operational amplifier has a finite and frequency-dependent gain $A(\omega)$. Second, the operational amplifier input capacitance, the sensor's output capacitance, and any additional parasitic capacitance created by connecters, cables, or printed circuit board (PCB) traces together form an input capacitance Cq. Third, feedback resistors R_f above several megaohms cannot be assumed to be ideal resistors anymore[4] and their parasitic capacitance C_f limits the circuit's bandwidth.[5] Typical values are a few picofarads for Cq and a few tens of femtofarads for *Cf*. The resulting transfer function assuming a high direct current open loop gain of the operational amplifier is given by Eq. (1).

$$\frac{V_{out}}{i} = -R_f \frac{1}{1 + j\omega R_f \left(C_f + \frac{C_q}{A(\omega)}\right)}. \tag{1}$$

It can be seen that all these effects together form one or more poles, limiting the bandwidth of the transimpedance amplifier. As a high value feedback resistor R_f is required to achieve the desired low noise,[6] it is necessary to minimize both the feedback and the input capacitance in order to achieve the desired bandwidth. Furthermore, a lower input capacitance Cq also leads to lower noise.[6] Typically, these optimizations alone are not sufficient to achieve the desired bandwidth and are therefore combined with a compensation network as shown in Refs. 5, 7, or 8, which tries to cancel the poles shown in Eq. (2) in order to achieve better bandwidth. However, in order to maintain a flat frequency response for the complete transimpedance amplifier, it is necessary that the poles and zeroes of this compensation network match the zeroes and poles of the original transfer function extremely well. Unfortunately, the non-ideal behavior of the feedback resistor is typically much more complicated than just exhibiting a single feedback capacitance creating a single pole. While

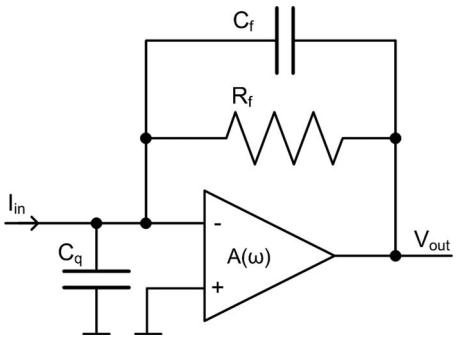

FIG. 1. Transimpedance amplifier with parasitic components.

this effect is often indistinguishable from the poles created by the input capacitance when looking at the transfer function, it becomes quite obvious in other problems. Depending on the operational amplifier's frequency response $A(\omega)$ and the values of the parasitic capacitances C_f and C_q, the circuit can exhibit excessive ringing or even become unstable. This problem is described by Eq. (2), giving the relationship between the output voltage V_{out} and the input voltage V_{in} of a non-inverting amplifier whose feedback network possesses the transfer function $B(\omega)$ from the operational amplifier's output to its inverting input. It is important to note that this transfer function only describes the stability of the transimpedance amplifier and is not directly related to the current to voltage transfer function.

$$\frac{V_{out}}{V_{in}} = \frac{A(\omega)}{1 + A(\omega) \cdot B(\omega)}. \tag{2}$$

As can easily be seen, the circuit becomes unstable if $A(\omega)$ multiplied by $B(\omega)$ equals minus one. Since they are both complex quantities, this is the case when their absolute values are reciprocal and their phase angles add up to a phase shift of 180°. Viewed from the output of the operational amplifier, the feedback resistor R_f and the input capacitance C_q form a first order low pass filter (PT1 system) for the voltage fed back to the inverting input. From the same perspective, the feedback resistor R_f and the feedback capacitance C_f act as a first order high pass filter (PD1 system). The respective corner frequencies of these filters are given by Eqs. (3) and (4).

$$f_{RfCq} = \frac{1}{2 \cdot \pi \cdot Rf \cdot Cq}, \tag{3}$$

$$f_{RfCf} = \frac{1}{2 \cdot \pi \cdot Rf \cdot Cf}. \tag{4}$$

As the input capacitance of an operational amplifier can be expected to be several picofarads, while the parasitic capacitance across a resistor is only about a hundred femtofarads for a 0805 SMD package, these corner frequencies will differ by at least a decade. Furthermore, unlike in the transimpedance transfer function given by Eq. (1), the input capacitance is not scaled by the operational amplifier gain $A(\omega)$. Therefore, the frequency response of the feedback network $B(\omega)$ can be expected to develop a −20 dB per decade slope between them as shown by the solid black line in Figure 2. In practice, however, large value resistor show a

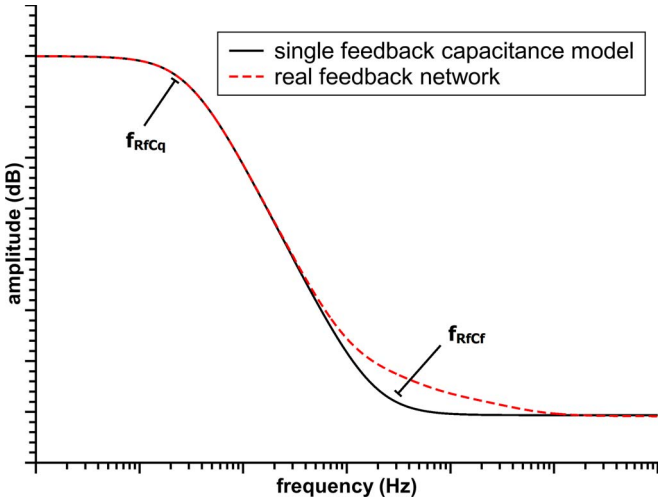

FIG. 2. Frequency response $B(\omega)$ of the feedback network with parasitic capacitances.

much more complicated non-ideal behavior, which has been described before in Refs. 4 and 6 but not explained. This results in the feedback network transfer function shown by the dashed red line in Figure 2, leading to a more complicated stability assessment and also to a more complicated transfer function.

Due to the high performance requirements on the operational amplifier, composite amplifiers using discrete input transistors or additional operational amplifiers are used in many cases, meaning that the frequency response of the operational amplifier $A(\omega)$ is typically not fixed but can be adjusted to maximize the performance. Furthermore, due to the increased number of amplifier stages, it contains more poles and zeroes than the transfer function of a single operational amplifier and is not necessarily unity-gain stable. At the same time, the frequency response of the feedback network $B(\omega)$, which depends on all the parasitic elements shown in Figure 1, is also subject to optimization and can change depending on the sensor connected to the input. The modification of some parts, for example, the input transistors, does even change both functions at the same time. Therefore, stability is not given in a complex transimpedance amplifier design but rather achieved by tuning both $A(\omega)$ and $B(\omega)$ to achieve high gain, high bandwidth, and low noise as well as stability.

Thus, a technique for measuring these parasitic elements is necessary in order to develop an optimized transimpedance amplifier, preferably a technique that allows measurements to be made while the amplifier is connected to the sensor. Furthermore, capacitance values as low as a few tens of femtofarads mean that every additional connection made for the measurement would add orders of magnitude more capacitance, rendering any calibration attempt in this case highly complicated. Due to these problems, just connecting a LCR meter to measure the parasitic capacitances in a transimpedance amplifier is not a viable option and the development of a more applicable measurement technique is necessary.

III. KNOWN METHODS

The simplest way possible to obtain knowledge about the feedback network is applying an alternating current to the input of the amplifier and measuring the resulting output voltage. By varying the frequency, the transfer function given by Eq. (1) can be obtained. However, as can be directly seen from Eq. (1) and Figure 2, the complexity of the overlapping pole(s) formed by the parasitic capacitances and the operational amplifier transfer function renders obtaining meaningful conclusions from these data near impossible unless several of these quantities are already well-known.

A more sophisticated approach is applying an alternating voltage to the non-inverting input of the operational amplifier and measuring the resulting output voltage. In this case, the input stage is not operated as a transimpedance amplifier but as a non-inverting voltage amplifier possessing the transfer function given by Eq. (2). Thus, the transfer function of the feedback network $B(\omega)$ can be directly obtained from this measurement as long as $A(\omega)B(\omega) \gg 1$. However, the region of interest for stability assessment is where $A(\omega)B(\omega)$ approaches 1, meaning that either $A(\omega)$ needs to be well-known or extrapolation from the data points at lower frequencies is necessary. While this extrapolation is possible as long as only a single low-frequency pole exists, this is not the case for real high value resistors, as can be seen in Figure 2.

Furthermore, regardless of these problems in obtaining accurate values, these methods suffer from a much more serious disadvantage. They both operate the transimpedance amplifier using its feedback network for feedback, meaning that they are only usable with an already stable combination of operational amplifier, feedback, and compensation network. However, information about the feedback transfer function is crucial for being able to successfully find a stable design in the first place.

IV. PROPOSED METHOD

In order to overcome these problems, we have developed a measurement technique that employs the first stage of the transimpedance amplifier for carrying out the measurement, but without operating it using its feedback network. This way, there is no difference at the critical circuit nodes between normal transimpedance amplifier operation and the feedback network transfer function measurement, allowing for very accurate measurements with simple tools and no need for additional calibration. However, as the transimpedance amplifier input stage is not operated using its feedback network, this measurement technique is unconditionally stable.

The basic setup is shown in Figure 3. One side of the feedback resistor has been disconnected from the output of the first stage operational amplifier and is instead driven by an input voltage V_{signal}. As parasitic capacitances on this side of the feedback resistor have no significant effect on the frequency response as long as the signal source has low output impedance, the additional capacitance of the input cable has no effect on the measurement. Furthermore, since the operational amplifier has a sufficiently low impedance output as well, it is not of interest to measure the parasitic capacitances on this node.

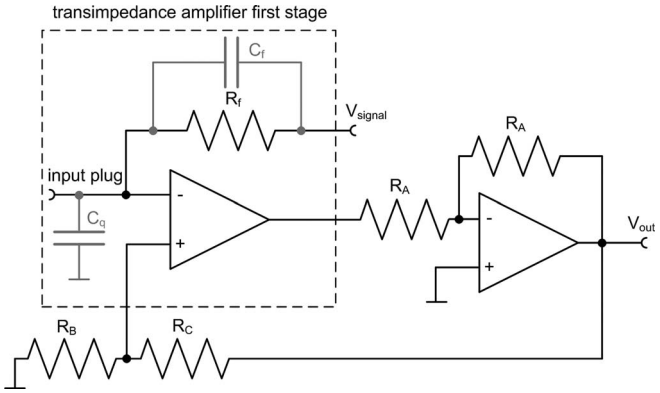

FIG. 3. Transimpedance amplifier modification for measuring parasitic elements.

The feedback resistor R_f, its parasitic capacitance C_f, and the parasitic input capacitance C_q form a frequency dependent voltage divider. Thus, if one of these quantities and the voltage on the inverting input of the first stage operational amplifier is known, the other two can be calculated from a measurement of the voltage across frequency. This calculation can both be carried out by finding the two corner frequencies or one corner frequency and the dampening ratio between the two constant amplitudes. As the resistance of the feedback resistor can be easily measured using an ohmmeter, the only missing quantity is the voltage.

Normally, a non-inverting amplifier configuration would be needed in order to measure the voltage created by the mentioned voltage divider with high input impedance. However, as the first stage operational amplifier's inverting input is connected to this circuit node, this is not directly possible. Therefore, we have added a second operational amplifier in an inverting configuration with unity gain. This inversion effectively interchanges the inverting and non-inverting input of the first stage operational amplifier with respect to the output voltage V_{out}, so that feeding this voltage back to the originally non-inverting input results in negative feedback and a stable loop. The additional voltage divider created by R_B and R_C sets the gain of this new non-inverting amplifier configuration. As none of the connections at the input connector have been changed, this circuit allows us to measure the capacitances as they are during transimpedance amplifier operation without actually operating the circuit as a transimpedance amplifier.

It is important to note that when using this circuit as a transimpedance amplifier, the second stage operational amplifier can be used as an inverting amplifier for additional gain. Therefore, adding this measurement setup to an amplifier requires only four extra components – the resistors R_B and R_C, the additional connector for the input voltage V_{signal}, and a solder bridge to separate one side of the feedback resistor from the output of the first stage operational amplifier for the feedback measurement.

V. EXPERIMENTAL

To verify this measurement technique, a printed circuit board with a transimpedance amplifier containing the circuit

described in Figure 3 was designed. As the feedback resistor R_f, a 1 GΩ resistor in a 0805 SMD package was used. Its value was measured using an Agilent 3458A digital multimeter. The input voltage V_{signal} for the feedback measurement was provided by an Agilent 81150A function generator, while the output voltage V_{out} was recorded by an Agilent DSO-X 3034A digital storage oscilloscope. For each frequency step, both the function generator output and the circuit output were measured to compensate for the frequency response of the measurement equipment. The ratio between the input signal and the output signal was then obtained from a FFT calculated across 30 periods of the averaged signals in order to increase the dynamic range. To ensure that the frequency response of the operational amplifiers in Figure 3 does not influence the measurement, the transfer function from the input plug to the output voltage has been measured, showing a flat gain across the frequency band of interest. In order to simulate different sensor capacitances, test fixtures consisting of high quality SMA connectors and precision ceramic capacitors were used. Their values were verified using an Agilent E4980A precision LCR meter.

Based on the knowledge gained from these measurements, an optimized transimpedance amplifier was assembled. Its frequency response was measured using a SFH250V photodiode, whose frequency response was verified using a commercial Femto DLPCA-200 transimpedance amplifier.

VI. RESULTS AND DISCUSSION

Using the experimental setup described above, the transfer function of the voltage divider formed by R_f, C_f, and C_q was acquired for several configuration. The red dots in Figure 4 show a measurement with cleaned PCB and open input plug, while the solid blue line is a fit of the analytical model from Figure 2 containing two first order systems. It is obvious that the model perfectly fits the first corner frequency, which corresponds to the feedback resistor R_f and the parasitic input capacitance C_q, but fits rather poorly at the second corner frequency, which corresponds to the feedback resistor

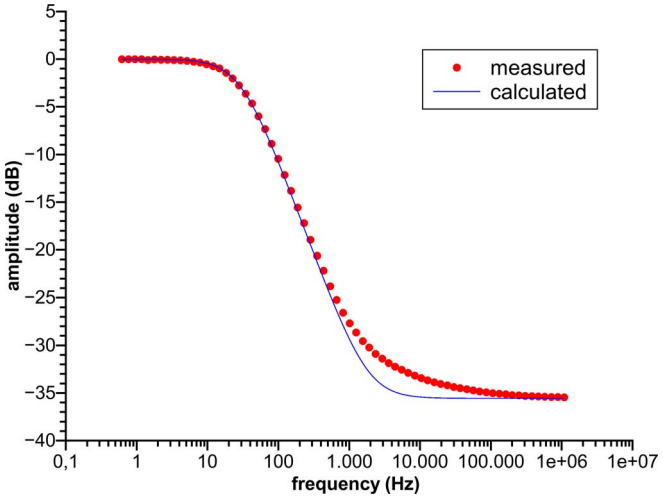

FIG. 4. Measurement with only the parasitic elements. This measurement results in a C_q of 5.1 pF and a C_f of 86 fF.

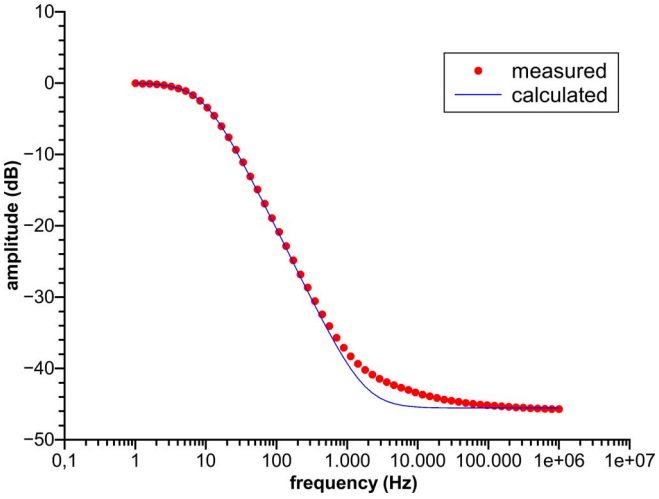

FIG. 5. Measurement with an additional 11 pF applied to the input plug. This measurement results in a C_q of 16.2 pF and a C_f of 86 fF.

R_f and its parasitic capacitance C_f. Such a non-ideal behavior of the feedback resistor was described in Refs. 4 and 6, but its source could not be explained. In order to obtain a value for the parasitic feedback capacitance C_f despite these non-idealities, we used the total dampening of 36 dB, which corresponds to the ratio between the two capacitances. This way, we calculated a parasitic input capacitance of 5.1 pF and a feedback capacitance of 86 fF. These two results fit the values that can be expected of an operational amplifier input and a 0805 SMD package respectively very well.

To verify our measurements, a capacitance of 11.1 pF was connected at the input plug, thus increasing the input capacitance C_q. Figure 5 shows the resulting measurement and a fit of the analytical model. This time, the calculations result in input capacitance of 16.2 pF and a feedback capacitance of 86 fF. Compared to the measurement shown in Figure 4, this is an increase in measured input capacitance of 11.1 pF, while the measured feedback capacitance did not change, thus proving that our method does indeed measure these capacitances correctly. However, this measurement shows the same shape at the second corner frequency, which differs from the shape expected from theory.

It should be noted that in this case, the necessary gain bandwidth product to stabilize the circuit has increased by a factor of three compared to Figure 4, as the final value of the transfer function has decreased by a factor of three. This emphasizes the necessity of minimizing the input capacitance. As the presented technique is able to measure the capacitance at the input accurately, it can also be used to optimize the layout of the sensor and the connection to the amplifier, which is especially useful in setups where sensors and amplifier are implemented as a single system. For example, we also used our transimpedance amplifier to optimize the faraday plate in our ion mobility spectrometer, as the amplifier is able to directly measure the capacitance of the entire setup.

In order to also verify the measurement regarding different feedback capacitances, we removed the additional input capacitance and soldered a 1 pF SMD 0805 capacitor directly

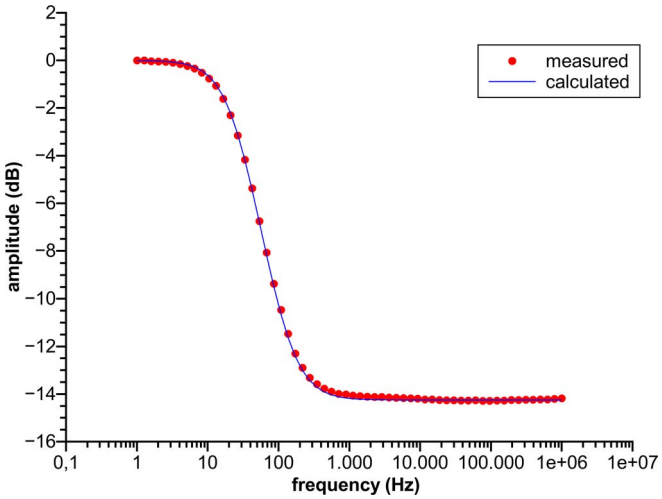

FIG. 6. Measurement with open input plug and 1 pF soldered onto the 1 GΩ feedback resistor. This measurement results in a C_q of 6.1 pF and a C_f of 1.18 pF.

onto the feedback resistor R_f. Figure 6 shows the results of this measurement, again together with an analytical fit. This fit results in a slightly increased input capacitance, possibly due to a change in the curve shape, and a feedback capacitance increase of 1.1 pF, which agrees very well with the expected value of 1 pF. It can be seen that the additional feedback capacitance has reduced the necessary gain bandwidth product to a tenth of its original value, thus stabilizing the circuit. Due to this effect, a small capacitance is often added across the feedback resistor to facilitate the design of low bandwidth transimpedance amplifiers. This is, however, not an option for high bandwidth designs, as the increased feedback capacitance also reduces the bandwidth of the current-to-voltage transfer function by the same factor.

Unlike in Figures 4 and 5, the analytical curve fits the measured points perfectly for all frequencies this time. As the difference between this and the other two measurements is the additional feedback capacitance, it is to be expected that the non-ideal behavior of the feedback resistor results from its parasitic capacitance. As these effects greatly influence nearly every part of the transimpedance amplifier design, it is important to gain a better understanding of how the parasitic elements interact with the resistor. We propose that the main cause for these non-idealities can be found in the shape of the resistive material itself. Most resistors in the high megaohm or gigaohm range are manufactured using thick film technology. In order to provide such high resistance in a package as small as 0805, the resistive material is not placed in a straight line, but in the shape of a meander as shown in the left panel of Figure 7. While this technique allows for compact high value resistors, it also creates parasitic capacitance inhomogeneously distributed across the resistor as shown by the electrical approximation of the meander in the right panel of Figure 7.

As there is no longer a single feedback resistor and a single parasitic capacitance, there is no longer one defined corner frequency. Instead, a multitude of poles and zeroes exist at closely spaced frequencies. Their superposition can result

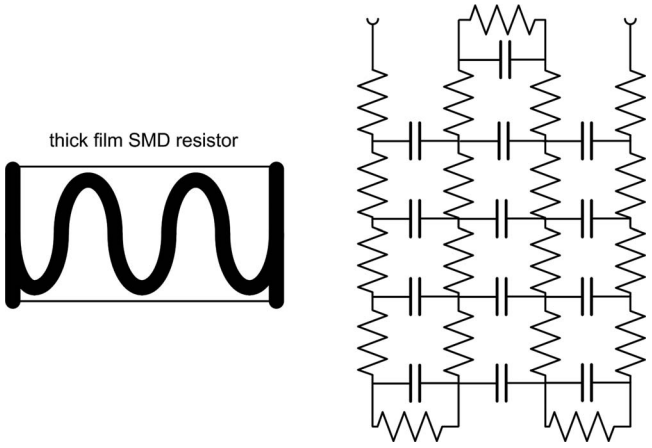

FIG. 7. Typical meander shape of a high resistance thick film resistor (left) and its electrical approximation (right).

in a much smoother shape than the frequency response of a first order system, as the frequency response of each pole or zero cannot fully develop before the next corner frequency is reached. In order to verify this theory, we setup different LTSpice simulations of the feedback network and compared the results with our measurements as shown in Figure 8.

The first simulation contained only one feedback resistor with a value of 1 GΩ and a single feedback capacitance in parallel. The result of this simulation is shown by the dashed blue line in Figure 8. As expected, the frequency response is exactly identical with the one obtained from the first order model in Figure 2 and fits the measured data poorly around the second corner frequency. To improve the accuracy of our model, we split the feedback resistor into 60 equal resistors, each having a resistance of $\frac{1}{60}$ GΩ. This way, each one of these resistors represents the same distance along the meander. However, the parasitic capacitances cannot all be equal, as the distance to the next loops of the meander varies depending on the position. Therefore, we used a capacity distribution corresponding to the shape of the meander as shown in Figure 7. The result of this simulation is shown as the solid

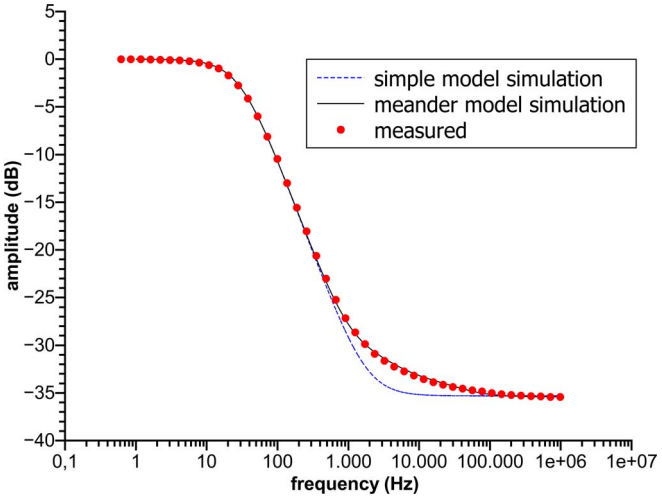

FIG. 8. Simulation of the simple circuit (dashed blue) and the meander model (black) compared to the measurement (red dots).

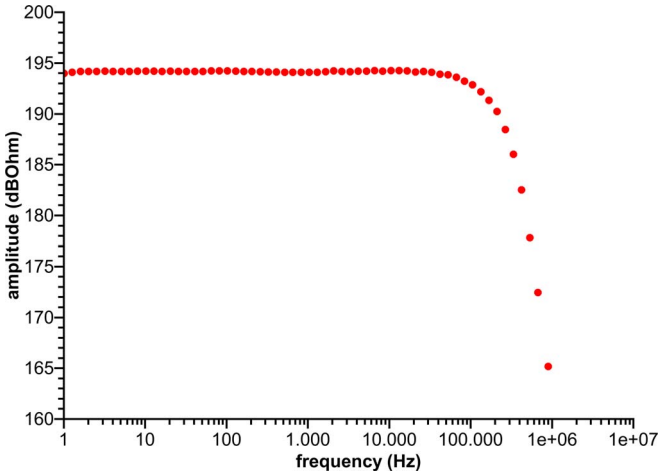

FIG. 9. Transfer function of our transimpedance amplifier with a flatness of ±100 mdB.

black line in Figure 8. This time, the simulation results fit the measured data perfectly, indicating that this is indeed an explanation for the observed, but so far unexplained non-ideal behavior of high value thick film resistors.

Based on the data we obtained from the feedback measurements, we also optimized the compensation network and the layout of the input stage of our transimpedance amplifier. This way, we were able to increase the feedback resistor to 1 GΩ and reduce the input capacitance to 5.1 pF, achieving a bandwidth of 175 kHz at a total transimpedance of 5 GΩ as shown in Figure 9. Furthermore, the total input-referenced current noise is only 9.7 pA. While this bandwidth is well above the second corner frequency of our feedback resistor at which the non-ideal behavior of its parasitic feedback capacitance begins to gain influence, as can be seen in Figure 8, the current-to-voltage transfer functions maintains a flatness of ±100 mdB.

VII. CONCLUSION

In this paper, we presented a method to directly and accurately measure the parasitic elements of a transimpedance amplifier by using its own input stage. Compared to other setups utilizing similar measurement schemes, our approach requires two extra resistors, but is in return able to measure the parasitic effects across the whole frequency range of interest and with unconditional stability. Using this technique, we were able to measure parasitic capacitances down to a few tens of femtofarads using only standard electronic laboratory equipment. The only required devices apart from the transimpedance amplifier itself are a function generator and an oscilloscope being able to generate and measure signals up to 1 MHz and an ohmmeter able to measure the value of the used feedback resistor. Furthermore, using the data obtained with this measurement technique in conjunction with a circuit simulation, we were able to give an explanation for the frequency response of the high value feedback resistors used in transimpedance amplifiers.

[1]G. Eiceman and Z. Karpas, *Ion Mobility Spectrometry* (CRC Press, 2005).
[2]A. Kirk, M. Allers, P. Cochems, J. Langejuergen, and S. Zimmermann, "A compact high resolution ion mobility spectrometer for fast trace gas analysis," Analyst **138**(18), 5200–5207 (2013).
[3]R. Mancini, *Op Amps for Everyone* (Texas Instruments, 2002).
[4]F. S. Goulding, J. Walton, and D. F. Malone, "An opto-electronic feedback preamplifier for high-resolution nuclear spectroscopy," Nucl. Instrum. Methods **71**(3), 273–279 (1969).
[5]D.-J. Kim and J.-Y. Koo, "A low-noise and wide-band ac boosting current-to-voltage amplifier for scanning tunneling microscopy," Rev. Sci. Intrum. **76**, 023703 (2005).
[6]G. De Geronimo, G. Bertuccio, and A. Longoni, "A low-noise wide-band transimpedance amplifier for current noise spectra measurements," Rev. Sci. Instrum. **67**, 2643 (1996).
[7]B. Michel, L. Novotny, and U. Dürig, "Low-temperature compatible I-V converter," Ultramicroscopy **42–44**, Part 2, 1647–1652 (1992).
[8]J. Jersch, F. Demming, I. Fedotov, and K. Dickmann, "Wide-band low-noise tunnel current measurements in laser assisted experiments," Rev. Sci. Instrum. **70**, 3173 (1999).